Available online at www.sciencedirect.com

ScienceDirect

International Journal of Solids and Structures 43 (2006) 7322–7336

INTERNATIONAL JOURNAL OF SOLIDS and STRUCTURES

www.elsevier.com/locate/ijsolstr

Grain size effects in multiphase steels assisted by transformation-induced plasticity

S. Turteltaub *, A.S.J. Suiker

Faculty of Aerospace Engineering, Delft University of Technology, Kluyverweg 1, 2629 HS Delft, The Netherlands

Received 10 October 2005; received in revised form 13 June 2006
Available online 20 June 2006

Communicated by Thomas Pardoen

Abstract

The influence of the austenitic grain size on the overall stress–strain behavior in a multiphase carbon steel is analyzed through three-dimensional finite element simulations. A recently developed multiscale martensitic transformation model is combined with a plasticity model to simulate the transformation-induced plasticity effects of a grain of retained austenite embedded in a ferrite-based matrix. Grain size effects are included via a surface energy term in the Helmholtz energy. Tensile simulations for representative orientations of the grain of retained austenite show that the initial stability of the austenite increases as the grain size decreases. Consequently, the effective strength is initially higher for smaller grains. The influence of the grain size on the evolution of the transformation process strongly depends on the grain orientation. For "hard" orientations, the transformation rate is higher for larger grains. In addition, the phase transformation is partially suppressed as the grain size decreases. In contrast, for "soft" orientations, the transformation rate is lower for larger grains. The phase transformation is more homogeneous for smaller grains and, consequently, the effective transformation strain is larger. Nevertheless, in multiphase carbon steels with a relatively low percentage of retained austenite, the influence of the austenitic grain size on the overall constitutive response is smaller than the influence of the austenitic grain orientation.

Keywords: Size effects; TRIP steel; Austenite; Martensitic phase transformation; Plasticity

1. Introduction

Among the class of high-strength high-ductility steels being developed, special attention has been devoted to low-alloyed steels whose microstructure at room temperature consists of a dispersed mixture of ferrite, bainite, thermal martensite and isolated grains of retained austenite. This class of multiphase steels can achieve high levels of strength without the addition of costly alloying elements such as Cr or Ni. The improved

* Corresponding author. Tel.: +31 15 2789552.
E-mail addresses: s.r.turteltaub@lr.tudelft.nl (S. Turteltaub), a.suiker@lr.tudelft.nl (A.S.J. Suiker).

0020-7683/$ - see front matter
doi:10.1016/j.ijsolstr.2006.06.017

mechanical performance of multiphase steels (compared to traditional carbon steels) has been attributed to a transformation-induced plasticity effect (TRIP effect) that occurs when the grains of retained austenite transform into martensite upon mechanical loading. Experimental studies have shown that an important factor that controls the performance of TRIP steels is the rate of transformation of austenite into martensite as a function of the deformation (i.e., the "stability" of austenite).

There are several factors that affect the transformation rate at the level of a grain of retained austenite. As shown in experimental studies (Oliver et al., 2002; Kruijver et al., 2003) and modeling analyses (Turteltaub and Suiker, 2005; Suiker and Turteltaub, 2005), the transformation rate in TRIP steels depends on the orientation of the grain with respect to the loading. A second factor that controls the transformation rate is the size of the grain of retained austenite. It has been experimentally observed in studies of fully austenitic alloys and multiphase TRIP steels that the resistance to martensitic transformation increases as the grain size of austenite decreases (Leal and Guimaraes, 1981; Jeong et al., 1993). The grain size of the retained austenite to some extent can be controlled through a suitably chosen thermal processing route (Bai et al., 1998). Consequently, in order to optimize the mechanical characteristics of TRIP steels, it is relevant to understand in detail the effect of the austenitic grain size on the onset and evolution of the martensitic transformation, which is the main objective of the present work.

In multiphase carbon steels, austenite can be found in several forms, namely as "blocky-type" grains and as "film-type" lamellaes intertwined with bainitic plates (Jeong et al., 1993; Jacques et al., 2001). The austenite present in the bainitic phase generally does not transform into martensite. In contrast, the blocky-type austenitic grains do transform upon application of mechanical loads. In the present study, attention will be focussed on the latter type of grains, i.e., retained austenite surrounded by a ferrite-based matrix. The thermomechanical response of retained austenite depends on sub-grain phenomena and length scales sketched in Fig. 1. In austenite to martensite phase transformations, the basic lattice structure changes from face-centered cubic (FCC) to body-centered tetragonal (BCT). At the lattice scale, the martensite consists of one out of three possible BCT variants. Two of these variants, arranged in specific proportions and orientations, form a twinned structure at the lower microscale that is termed a "transformation system". The type of martensite that we consider in the present analysis is twinned plate martensite. Thermally induced plate martensite is associated to a high value of carbon concentration of 1.4 wt.% and higher in the austenitic parent phase (Umemoto et al., 1983; Christian, 2002). Experimental studies have indicated the appearance of twinned martensite upon mechanical loading in TRIP steels with a local value of carbon concentration of 1.4 wt.% and higher in the grains of retained austenite (Sugimoto et al., 1997; Rao and Rashid, 1997). As a working assumption, we consider that the mechanically induced martensite is similar to the thermally induced martensite for the same carbon concentration. According to the theory of martensitic phase transformations (Wechsler et al., 1953; Ball

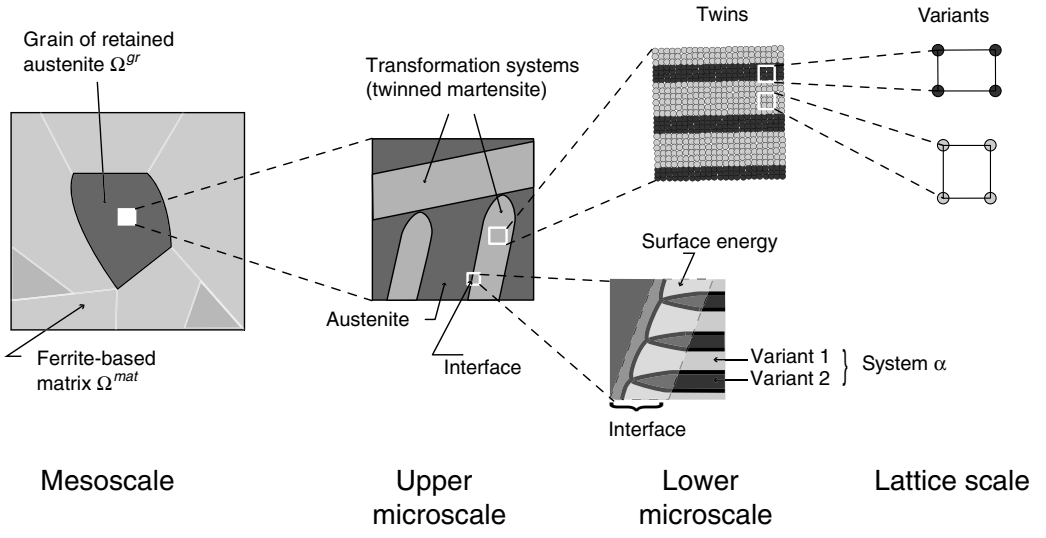

Fig. 1. Sub-grain structures and length scales.

and James, 1987), there are 24 possible stress-free martensitic transformation systems. At the upper microscale, a grain of retained austenite contains platelets of twinned martensite intertwined with untransformed austenite. In the present context, the mesoscale refers to a representative sample containing austenite and possibly several transformation systems of martensite.

Various models have been proposed for transformation-induced plasticity but only a few of them address the issue of grain size effects. Adopting a geometrically linear framework, Reisner et al. (1998) studied the transformation rate in a Cu–Fe and a low-alloyed TRIP steel, although grain size effects were only included for the Cu–Fe alloy. They predicted that the number of alternating bands of martensitic twins increases with increasing grain size. Based on a modification of a model proposed by Olson and Cohen (1975) and applying the Hall–Petch relation for the austenitic phase, Iwamoto and Tsuta (2000) studied the influence of grain size on the mechanical response of an austenitic stainless steel. Their phenomenological model, which does not explicitly take into account the crystallography of the transformation systems, predicts an increase in effective tensile strength for an increase in austenitic grain size. This result is ascribed to the formation of less martensite for smaller grain sizes. Also based on a modification of the Olson-Cohen model, Perlade et al. (2003) proposed a one-dimensional constitutive formulation for low-alloyed TRIP steels. The effective strength resulting from stress-assisted and strain-induced transformations was found to be sensitive to the austenitic grain size.

In the present study, we assume that plastic deformations occur primarily in the ferrite-based matrix while the untransformed austenite behaves elastically. Although the austenite adjacent to a newly formed platelet of martensite deforms plastically to accommodate the transformation strain, we assume that this plastic deformation is confined to a small neighborhood around the martensite and that the stresses in the rest of the austenite (bulk) remain below the initial yield strength. The small scale yielding assumption is reasonable for austenite with a relatively high carbon concentration, which has a high yield strength in comparison with the ferrite-based matrix (Furnémont et al., 2002). The effect of the local plastic accommodation is lumped into the transformation barrier at the mesoscale. The validity of this assumption is limited to stresses in the grain that are below the initial yield strength of the austenite. However, in many common grades of multiphase TRIP steels, the austenitic phase deforms plastically before transformation. For those steels, the assumption of an elastic austenitic phase will probably affect the quantitative predictions of the model considered in the present communication. Nonetheless, the predicted trends are expected to be essentially correct. The influence of the plastic deformation in the austenite will be analyzed in forthcoming work.

The effects of austenitic sub-grain structures on the kinematics and the constitutive behavior are accounted for using a recently developed multiscale model for martensitic transformations (Turteltaub and Suiker, 2005, 2006; Suiker and Turteltaub, 2005). The microstructural information for the phase transformation model is based on the crystallographic theory of martensitic transformations and further includes the anisotropic stiffness of each system of twinned martensite. In addition, the model contains a surface energy term associated to regions close to the habit planes, as shown at the upper and lower microscales in Fig. 1. The surface energy is indirectly related to the grain size via a length scale parameter. Using this feature of the model, it is possible to study the effect of grain size on the mesoscale responses of a TRIP steel.

A summary of the transformation model is given in Section 2, with a microstructural interpretation of the length scale parameter introduced in the surface energy. Simulations of grain size effects are presented in Section 3, where the response for several grains sizes is analyzed for two representative orientations of the grain of retained austenite. Finally, in Section 4, some closing remarks are given. As a general scheme of notation, scalars are written as lightface italic letters (e.g., a, b), vectors as boldface lowercase letters (e.g., $\boldsymbol{a}$, $\boldsymbol{b}$), second-order tensors as boldface uppercase letters (e.g., $\boldsymbol{A}$, $\boldsymbol{B}$) and fourth-order tensors as blackboard bold capital letters (e.g., $\mathbb{A}, \mathbb{B}$). For vectors and tensors, Cartesian components are denoted as a_i, A_{ij} and A_{ijkl}. The action of a second-order tensor on a vector is denoted as $\boldsymbol{Ba}$ (in components $B_{ij}a_j$, with implicit summation on repeated indices) and the action of a fourth-order tensor on a second-order tensor is denoted as $\mathbb{B}\boldsymbol{A}$ (i.e., $B_{ijkl}A_{kl}$). Composition of two second-order tensors is denoted as $\boldsymbol{AB}$ (i.e., $A_{ij}B_{jk}$). The tensor product between two vectors is denoted as $\boldsymbol{a} \otimes \boldsymbol{b}$ (i.e., a_ib_j). All inner products are denoted with a single dot between tensorial quantities of the same order, i.e., $\boldsymbol{a} \cdot \boldsymbol{b}$ for vectors and $\boldsymbol{A} \cdot \boldsymbol{B}$ for second-order tensors (in components, a_ib_i and $A_{ij}B_{ij}$ respectively). A material time derivative is denoted by a superimposed dot.

2. Transformation model

Martensitic transformations (FCC to BCT) in multiphase carbon steels are characterized by the formation of up to 24 active transformations systems. A transformation system is denoted with a superscript α. Each transformation system is described in terms of a shape strain vector $\boldsymbol{b}^{(\alpha)}$ and the unit vector normal to the habit plane $\boldsymbol{m}^{(\alpha)}$ (i.e., a vector normal to the austenite-twinned martensite interface). The shape strain vector can be expressed as

$$\boldsymbol{b}^{(\alpha)} = \gamma_T \hat{\boldsymbol{b}}^{(\alpha)},$$

where $\hat{\boldsymbol{b}}^{(\alpha)}$ is a unit vector in the direction of $\boldsymbol{b}^{(\alpha)}$ and $\gamma_T = |\boldsymbol{b}^{(\alpha)}|$ is the magnitude of the shape strain vector. The magnitude γ_T is the same for all 24 transformation systems (Wechsler et al., 1953; Ball and James, 1987).

Within the framework of large deformations, the mesoscale deformation gradient $\boldsymbol{F}$ in a material point of a grain of retained austenite may be decomposed as

$$\boldsymbol{F} = \boldsymbol{F}_{\mathrm{e}} \boldsymbol{F}_{\mathrm{tr}}, \tag{1}$$

where $\boldsymbol{F}_{\mathrm{e}}$ is the elastic deformation gradient and $\boldsymbol{F}_{\mathrm{tr}}$ is the transformation deformation gradient. Based on this decomposition, it is possible to introduce three configurations, namely the reference, intermediate and current configurations. In the present model, the mesoscale transformation deformation gradient in (1) is obtained through averaging lower scale kinematic information derived from the theory of martensitic transformations (Wechsler et al., 1953; Ball and James, 1987). This procedure leads to the following expression for the transformation deformation gradient (Turteltaub and Suiker, 2006):

$$\boldsymbol{F}_{\mathrm{tr}} = \boldsymbol{I} + \sum_{\alpha=1}^{N} \xi^{(\alpha)} \boldsymbol{\gamma}^{(\alpha)},$$

where

$$\boldsymbol{\gamma}^{(\alpha)} = \gamma_T \hat{\boldsymbol{b}}^{(\alpha)} \otimes \boldsymbol{m}^{(\alpha)}$$

is the transformation strain, $\xi^{(\alpha)}$ is the volume fraction of the transformation system α in the undeformed reference configuration, $N\,(=24)$ refers to the total number of transformation systems and $\boldsymbol{I}$ is the second-order identity tensor.

The constitutive relation between the second Piola–Kirchhoff stress $\boldsymbol{S}$ in the intermediate configuration and the elastic Green–Lagrange strain $\boldsymbol{E}_{\mathrm{e}} = (\boldsymbol{F}_{\mathrm{e}}^{\mathrm{T}} \boldsymbol{F}_{\mathrm{e}} - \boldsymbol{I})/2$ is taken as

$$\boldsymbol{S} = \mathbb{C} \boldsymbol{E}_{\mathrm{e}}, \tag{2}$$

where the mesoscopic effective stiffness tensor $\mathbb{C}$ has the form (Turteltaub and Suiker, 2005, 2006; Suiker and Turteltaub, 2005)

$$\mathbb{C} = \frac{1}{J_{\mathrm{tr}}} \left\{ \left(1 - \sum_{\alpha=1}^{N} \xi^{(\alpha)} \right) \mathbb{C}^{A} + (1 + \delta_T) \sum_{\alpha=1}^{N} \xi^{(\alpha)} \mathbb{C}^{(\alpha)} \right\}. \tag{3}$$

In (3), $\delta_T = \boldsymbol{b}^{(\alpha)} \cdot \boldsymbol{m}^{(\alpha)}$ is the volumetric expansion due to the phase transformation (same for all systems α) and $J_{\mathrm{tr}} = \det \boldsymbol{F}_{\mathrm{tr}}$. The terms $\mathbb{C}^{A}$ and $\mathbb{C}^{(\alpha)}$ refer to, respectively, the microscale stiffnesses of austenite and transformation system α of martensite. In turn, $\mathbb{C}^{(\alpha)}$ can be related to the stiffness of each variant of martensite and its orientation in the transformation system. Expressions for $\mathbb{C}^{(\alpha)}$ can be found in Turteltaub and Suiker (2006).

The Helmholtz energy $\hat{\psi}$ for the transformation model developed by Turteltaub and Suiker (2006) consists of a mesoscale bulk strain energy ψ_{m}, thermal contributions ψ_{th} and ψ_{h} and, central to the analysis of grain size effects, a surface energy term ψ_{s} that depends on the volume fractions $\xi^{(\alpha)}$ of the transformation systems. The general form of the Helmholtz energy density is

$$\hat{\psi}(\boldsymbol{E}_{\mathrm{e}}, \theta, \boldsymbol{\xi}) = \psi_{\mathrm{m}}(\boldsymbol{E}_{\mathrm{e}}, \boldsymbol{\xi}) + \psi_{\mathrm{th}}(\theta, \boldsymbol{\xi}) + \psi_{\mathrm{s}}(\boldsymbol{\xi}) + \psi_{\mathrm{h}}(\boldsymbol{\xi}), \tag{4}$$

where θ is the temperature and $\boldsymbol{\xi}$ is an N-dimensional vector whose entries are the martensitic volume fractions $\xi^{(\alpha)}$. In the isothermal analyses presented in this paper, specific forms for ψ_{th} and ψ_{h} are not necessary apart

from the fact that these energies are assumed to be linear functions of $\boldsymbol{\xi}$. The bulk elastic strain energy associated to the constitutive relation (2) has been derived as (Turteltaub and Suiker, 2006)

$$\psi_{\mathrm{m}}(\boldsymbol{E}_{\mathrm{e}},\boldsymbol{\xi}) = \frac{J_{\mathrm{tr}}(\boldsymbol{\xi})}{2\rho_0}\mathbb{C}(\boldsymbol{\xi})\boldsymbol{E}_{\mathrm{e}}\cdot\boldsymbol{E}_{\mathrm{e}}, \tag{5}$$

where ρ_0 is the mass density in the reference configuration. As shown in Fig. 1, at the lower microscale a local elastic deformation is required to preserve the coherency at the interface between austenite and twinned martensite (i.e., at the habit plane). A local strain energy can be associated to this deformation. In the model developed by Turteltaub and Suiker (2005, 2006), this contribution is not taken into account at the bulk level, but it is described via a mesoscale surface energy term (per unit mass) of the form

$$\psi_{\mathrm{s}}(\boldsymbol{\xi}) = \frac{\chi}{\rho_0 l_0}\sum_{\alpha=1}^{N}\xi^{(\alpha)}(1-\xi^{(\alpha)}). \tag{6}$$

Here, χ is an interface energy per unit area and l_0 is a length scale parameter. The above expression for the surface energy assumes that all austenite-twinned martensite interfaces have the same energy per unit area. The formulation given by (6) is based on a martensite–austenite interfacial area per unit volume that is proportional to the term $\xi^{(\alpha)}(1-\xi^{(\alpha)})$ for each transformation system α. This form is motivated from the following limit cases: (i) when there is no martensite present at a given material point (i.e., $\xi^{(\alpha)}=0$ for all α), the surface energy should be equal to zero, and (ii) when a given material point is fully occupied by a single martensitic transformation system (i.e., $\xi^{(\beta)}=1$, $\xi^{(\alpha)}=0$ for all $\alpha\neq\beta$), the surface energy should be equal to zero.

Observe that the surface energy shown in (6) refers only to the interfaces between twinned martensite and austenite (i.e., habit planes) and it does not include the energy associated to the interfaces between individual variants inside a transformation system (i.e., twins' surface energy). Under the assumption that the ratio between the surface occupied by the twins' interfaces and the volume occupied by the corresponding transformation system is constant, the energy associated to the twins' interfaces can be modeled as a linear function of the volume fraction. In contrast to the surface energy associated to the habit planes, an energy associated to the twins' interfaces would not be zero when $\xi^{(\beta)}=1$ for one given system β. In an analysis where individual values of $\xi^{(\beta)}$ become large (say, above 0.2), then an additional term related to the surface energy of the twins should be included in (6). Nonetheless, in the simulations shown in Section 3 below, none of the individual values of the volume fractions after completion of transformation was large and, for simplicity, the energy related to the twins' interfaces was not included.

One limitation of using the volume fraction of martensite as the independent variable for describing the surface energy is that it is implicitly assumed that at a material point there is only one platelet of each martensitic transformation system. The case where the volume fraction corresponds to two or more platelets of the same system is not accounted for. Furthermore, for simplicity, it is assumed that the interface energy per unit area between two transformation systems is 2χ; hence when two transformation systems coalesce, the expression (6) remains unaltered. Despite these simplifications, the expression for the surface energy is qualitatively in accordance with experimental observations reported by Leal and Guimaraes (1981) for an austenitic alloy.

An interpretation of the length scale parameter l_0 can be obtained from the geometry of a plate of twinned martensite inside a grain of austenite at the onset of transformation (i.e., when $\xi^{(\alpha)}\ll 1$). In particular, the value l_0 can be interpreted as the ratio between the initial volume and surface of a newly formed plate of twinned martensite (Turteltaub and Suiker, 2006). Accordingly, consider an ideal spherical grain of retained austenite with diameter d_0 and, at the beginning of the transformation, an ideal disc-shaped plate of twinned martensite of thickness t_0 that spans the whole grain, as shown in Fig. 2. The ratio between the volume and the surface of the martensitic platelet is

$$l_0 \approx \frac{\pi d_0^2 t_0}{4}\times\left(2\frac{\pi d_0^2}{4}\right)^{-1} = \frac{t_0}{2}, \tag{7}$$

where the surface $\pi d_0 t_0$ associated to the edge of the platelet has been neglected since typically the thickness of the platelet is much smaller than the diameter. For simplicity, the ratio $c=t_0/d_0$ of a plate of newly formed twinned martensite is assumed to be the same for all grain sizes d_0 (thus, the thickness t_0 changes proportionally

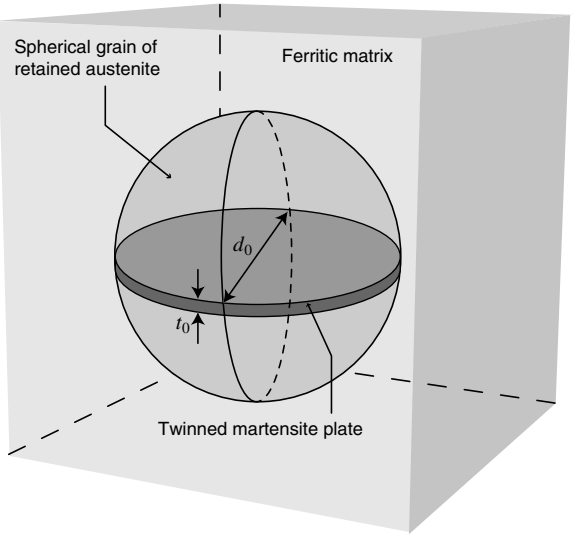

Fig. 2. Ideal disk-shaped platelet of martensite in an spherical grain of retained austenite.

with d_0). Therefore, from (7), the length scale parameter l_0 can be related to the average size d_0 of a grain of retained austenite and the ratio c as

$$l_0 \approx (c/2)d_0. \tag{8}$$

The expression for the surface energy given in (6) indicates that the martensite–austenite interfacial area per unit volume is inversely proportional to the length scale parameter l_0. Consequently, the interpretation of the length parameter given in (8) implies that the martensite–austenite interfacial area per unit volume is inversely proportional to the austenitic grain size d_0. This assumption is qualitatively consistent with the experimental observations of Leal and Guimaraes (1981) for fine and coarse grains in a Fe–Ni–C alloy.

The final ingredient of the transformation model consists of a constitutive relation that relates the rate of change of the martensitic volume fraction $\dot{\xi}^{(\alpha)}$ of system α to the corresponding transformation driving force $f^{(\alpha)}$. The transformation driving force $f^{(\alpha)}$ that is consistent with the Helmholtz energy given in (4) has been derived as (Turteltaub and Suiker, 2006)

$$f^{(\alpha)} = f_{\mathrm{m}}^{(\alpha)} + f_{\mathrm{s}}^{(\alpha)} + f_{\mathrm{th}}^{(\alpha)} \tag{9}$$

for $\alpha = 1, \ldots, N$, where

$$f_{\mathrm{m}}^{(\alpha)} := J_{\mathrm{tr}} \boldsymbol{F}_{\mathrm{e}}^{\mathrm{T}} \boldsymbol{F}_{\mathrm{e}} \boldsymbol{S} \boldsymbol{F}_{\mathrm{tr}}^{-\mathrm{T}} \cdot \boldsymbol{\gamma}^{(\alpha)} + \frac{1}{2}\left(\mathbb{C}^{A} - (1+\delta_T)\mathbb{C}^{(\alpha)}\right)\boldsymbol{E}_{\mathrm{e}} \cdot \boldsymbol{E}_{\mathrm{e}} \tag{10}$$

is the mechanical bulk contribution to the driving force that contains the resolved stress and a term related to the stiffness difference of the austenitic parent phase and the martensitic product phase. Furthermore,

$$f_{\mathrm{s}}^{(\alpha)} := -\frac{\chi}{l_0}(1 - 2\xi^{(\alpha)}) \tag{11}$$

is the surface energy contribution to the driving force, which reflects the creation (or annihilation) of interfaces (austenite–martensite and martensite–martensite). The thermal contribution to the driving force $f_{\mathrm{th}}^{(\alpha)}$ is constant for isothermal processes. The specific expression for $f_{\mathrm{th}}^{(\alpha)}$ can be found in Turteltaub and Suiker (2006).

Transformation occurs if the driving force $f^{(\alpha)}$ in (11) exceeds a critical value f_{cr}. The evolution of the transformation from austenite to a system α of martensite is taken to be governed by the following kinetic relation between rate of change of the martensitic volume fraction $\dot{\xi}^{(\alpha)}$ and the transformation driving force $f^{(\alpha)}$:

$$\dot{\xi}^{(\alpha)} = \dot{\xi}_{\max} \tanh\left(\frac{1}{v}\frac{\langle f^{(\alpha)} - f_{\mathrm{cr}}\rangle}{f_{\mathrm{cr}}}\right), \tag{12}$$

where $v > 0$ and $\dot{\xi}_{\max} \geqslant 0$ are a dimensionless viscosity-like parameter and the maximum value for the transformation rate, respectively. Further, Macauley brackets are defined as $\langle a \rangle := (|a| + a)/2$. The kinetic relation (12) is a phenomenological expression consistent with the framework of irreversible thermodynamics proposed by Onsager that relates a flux $\dot{\xi}^{(\alpha)}$ to an affinity $f^{(\alpha)}$ (see, e.g., Callen, 1985). Although the relation (12) is formally related to rate-dependent kinetics (that describe isothermal transformations), the parameters v and $\dot{\xi}_{\max}$ were calibrated to approximate the limit case of rate-independent kinetics (that describe athermal transformations, see Turteltaub and Suiker, 2005).

3. Grain size effects

3.1. Numerical simulations

To examine the influence of the grain size on the TRIP effect in carbon steels, several quasi-static uniaxial loading simulations were conducted on a polyhedral grain of retained austenite Ω^{gr} embedded in a ferrite-based matrix Ω^{mat}, as shown in Fig. 3. The grain of retained austenite occupies 16% of the total volume, which is a typical average value for multiphase TRIP steels (Jacques et al., 2001). The transformation model outlined in the previous section is used to simulate the mechanical response of the grain Ω^{gr}. For simplicity, the elasto-plastic response of the ferrite-based matrix Ω^{mat} is modelled by a large-strain, J_2-plasticity formulation with isotropic hardening. Although at the present scale of observation it would be more appropriate to use an anisotropic elastic model and an (anisotropic) crystal plasticity model, recent simulations have shown that a J_2-plasticity model provides similar results as a matrix composed of six ferritic single crystal grains with Euler angles evenly distributed in the orientation space (Tjahjanto et al., 2006). Within the framework of large deformation plasticity, the deformation gradient in a material point inside the ferrite-based matrix Ω^{mat} is decomposed as $\boldsymbol{F} = \boldsymbol{F}_{\mathrm{e}}\boldsymbol{F}_p$ where $\boldsymbol{F}_p$ is the plastic deformation gradient. The relation between the second Piola–Kirchhoff stress $\boldsymbol{S}$ in a stress-free intermediate configuration and the elastic Green–Lagrange strain $\boldsymbol{E}_{\mathrm{e}}$ is taken as

$$\boldsymbol{S} = \mathbb{C}^{\mathrm{F}}\boldsymbol{E}_{\mathrm{e}},$$

where $\mathbb{C}^{\mathrm{F}}$ is the stiffness tensor of the ferrite-based material and it is taken to be isotropic.

The computational domain $\Omega = \Omega^{\mathrm{gr}} \cup \Omega^{\mathrm{mat}}$ corresponds to a $3L \times 3L \times 3L$ cube aligned with a global basis $\{\boldsymbol{f}_1, \boldsymbol{f}_2, \boldsymbol{f}_3\}$ as shown in Fig. 3. The imposed boundary conditions simulate a uniaxial tensile test. The normal displacement of the top surface in the loading direction $\boldsymbol{f}_1$ is increased from 0 to 0.3 L which implies that the

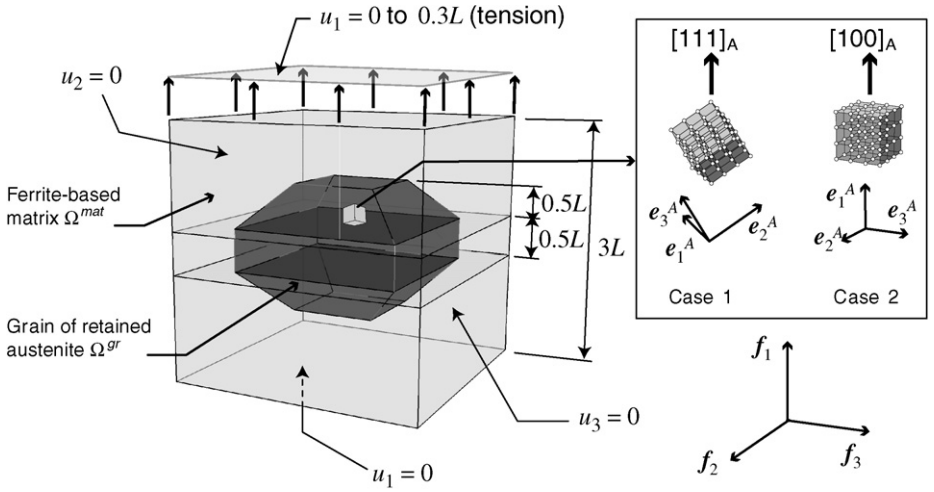

Fig. 3. Grain of retained austenite Ω^{gr} in a ferrite-based matrix Ω^{mat}. The inset indicates the different grain orientations.

final nominal uniaxial strain is 10%. The nominal strain rate is $10^{-4}\,s^{-1}$, which reflects quasi-static loading conditions. Further, the normal displacements of three mutually perpendicular faces are constrained and the remaining boundary conditions correspond to zero stress.

Two representative orientations for the grain of retained austenite were analyzed. The orientations are indicated in Table 1 in terms of the Euler angles that map the global basis $\{\boldsymbol{f}_1, \boldsymbol{f}_2, \boldsymbol{f}_3\}$ onto the lattice basis of austenite $\{\boldsymbol{e}_1^A, \boldsymbol{e}_2^A, \boldsymbol{e}_3^A\}$, as shown in the inset in Fig. 3. The Euler angles are given using the so-called "323" convention. For each orientation, Table 1 also provides the Miller indices of the loading direction $\boldsymbol{f}_1$ in the austenitic lattice basis. Henceforth, for ease of reference, the orientation of the grain will be referred to using the Miller indices of $\boldsymbol{f}_1$.

For each orientation of austenite, three different grain sizes were considered. The basic parameters related to grain size are summarized in Table 2. Taking into account that grains of retained austenite of the blocky-type in multiphase steels are in the range of 0.5 μm to a few microns (Jeong et al., 1993; Bai et al., 1998; Jacques et al., 2001), the analyses were carried out for grains of retained austenite with diameters d_0 as given in Table 2. The grain of austenite shown in Fig. 3 has a rectangular base of side length $2L$, which is taken to represent the grain size, i.e., $d_0 = 2L$. The side length $3L$ of the computational domain is indicated in the second column of Table 2. The third column of the table contains the corresponding values of the length scale parameter l_0 computed from (8) based on a fixed aspect ratio c, which has been estimated to be about $c = 0.05$ (Wang and van der Zwaag, 2001). Table 2 also includes the values of the ratio χ/l_0 that appears in the transformation driving force f_s given in (11). This ratio was computed based on a surface energy per unit area that, for martensitic transformations in metals and alloys, has been estimated to be $\chi = 0.2\,J\,m^{-2}$ (Christian, 2002).

Values for $\mathbb{C}^A$ and $\mathbb{C}^{(\alpha)}$ were obtained from nanoindentation tests carried out by Furnémont et al. (2002) following the interpretation presented in Turteltaub and Suiker (2005). The specific values can be found in Suiker and Turteltaub (2005) and, for brevity, will not be reproduced here. The values of the parameters used in the kinetic relation (12) have been chosen as $v \approx 0.17$, $\dot{\xi}_{\max} \approx 3 \times 10^{-3}\,s^{-1}$, which, under quasi-static conditions, reflect a weak rate-dependent transformation behavior (i.e., close to a rate-independent transformation behavior). Furthermore, the difference $f_{cr} - f_{th}$ between the critical value and the thermal contribution of the driving force has been estimated to be about 5 MPa (Turteltaub and Suiker, 2005).

Parameters for the ferrite-based material were calibrated from uniaxial tensile tests performed by Jacques et al. (2001) on a polycrystalline material composed of 75 wt.% ferrite and 25 wt.% thermal martensite. The calibration corresponds to an exponentially saturating hardening curve with an initial yield stress of 300 MPa and an ultimate yield stress in the saturated state of 880 MPa. More details on the calibration can be found in Suiker and Turteltaub (2005) and are not included here. For the analysis of grain size effects, it is important to point out that the ferrite has the lowest effective stiffness, followed by the austenite and finally the martensite (Furnémont et al., 2002).

Table 1
Orientations of grain of retained austenite given in terms of "323" Euler angles and corresponding loading direction given in Miller indices

Case	Orientation of austenite	Global loading direction $\boldsymbol{f}_1$
1	(45°, 36.26°, 0°)	$[1\,1\,1]_A$
2	(0°, 0°, 0°)	$[1\,0\,0]_A$

Table 2
Average grain size d_0 of austenite, side length $3L$ of computational domain, length scale parameter l_0 for an aspect ratio $c = 0.05$ and surface energy χ over l_0 for a surface energy of $0.2\,J\,m^{-2}$

d_0 [μm]	$3L$ [μm]	l_0 [μm]	χ/l_0 [MPa]
0.5	0.75	0.0125	16
2	3	0.05	4
8	12	0.2	1

The results obtained from the simulations are reported in terms of the Cauchy stress $\boldsymbol{T}$ in the current configuration and the logarithmic strain $\boldsymbol{e}$, which are defined as

$$\boldsymbol{T} := (\det \boldsymbol{F}_{\mathrm{e}})^{-1} \boldsymbol{F}_{\mathrm{e}} \boldsymbol{S} \boldsymbol{F}_{\mathrm{e}}^{\mathrm{T}}, \quad \boldsymbol{e} := \ln \boldsymbol{V},$$

where $\boldsymbol{V}$ is the left stretch tensor in the polar decomposition of the deformation gradient, i.e., $\boldsymbol{V} = \boldsymbol{F}\boldsymbol{Q}^{-1}$. The axial Cauchy stress component T_{11} averaged over the austenitic grain in the current configuration is

$$\overline{T}_{11}^{\mathrm{gr}} := \frac{1}{|\Omega_t^{\mathrm{gr}}|} \int_{\Omega_t^{\mathrm{gr}}} T_{11} \, \mathrm{d}v,$$

where Ω_t^{gr} is the region occupied by the austenitic grain in the current configuration at time t and the components are referred to the global basis $\{\boldsymbol{f}_1, \boldsymbol{f}_2, \boldsymbol{f}_3\}$. The axial Cauchy stress component T_{11} averaged over the whole computational domain in the current configuration is

$$\overline{T}_{11} := \frac{1}{|\Omega_t|} \int_{\Omega_t} T_{11} \, \mathrm{d}v,$$

where Ω_t is the region occupied by the computational domain Ω in the current configuration at time t. The axial logarithmic strain component e_{11} averaged over the austenitic grain in the reference configuration is given by

$$\bar{e}_{11}^{\mathrm{gr}} := \frac{1}{|\Omega_0^{\mathrm{gr}}|} \int_{\Omega_0^{\mathrm{gr}}} e_{11} \, \mathrm{d}v,$$

where Ω_0^{gr} is the region occupied by the austenitic grain in the reference configuration. The axial logarithmic strain component e_{11} averaged over the whole domain in the reference configuration is defined as

$$\bar{e}_{11} := \frac{1}{|\Omega_0|} \int_{\Omega_0} e_{11} \, \mathrm{d}v,$$

where Ω_0 is the region occupied by the whole computational domain in the reference configuration. The austenitic volume fraction ξ_A averaged over the whole domain in the reference configuration is given by

$$\bar{\xi}_A := \frac{1}{|\Omega_0|} \int_{\Omega_0^{\mathrm{gr}}} \left(1 - \sum_{\alpha=1}^{N} \xi^{(\alpha)} \right) \mathrm{d}v,$$

where $\xi^{(\alpha)}$ are the volume fractions of the martensitic transformation systems.

The computational domain was discretized using 1771 linear tetrahedrons. The transformation model was implemented using a fully implicit backward Euler discretization scheme for the stress update within the framework of finite deformations. A robust search algorithm was used in the return mapping algorithm for detecting the transformation systems activated during loading. Moreover, a sub-stepping algorithm was implemented to warrant the stability of the numerical update procedure, as well as to accurately satisfy the completion of the transformation process. The computation of the consistent tangent operator was performed through a numerical differentiation method. Details on the numerical implementation can be found in Suiker and Turteltaub (2005).

The effect of the grain size is analyzed in terms of (i) the stress–strain response at the level of the grain of retained austenite, (ii) the evolution of the phase transformation, (iii) the distribution of strains in the grain, and (iv) the stress–strain response of the whole domain Ω.

3.2. Size effects at the level of the grain of retained austenite

The grain-averaged axial Cauchy stress $\overline{T}_{11}^{\mathrm{gr}}$ as a function of the grain-averaged axial logarithmic $\bar{e}_{11}^{\mathrm{gr}}$ is shown in Figs. 4a and b when the grain of retained austenite in the matrix is loaded in the $[1\,1\,1]_A$ and the $[1\,0\,0]_A$ directions, respectively. It can be observed that the stress level at which the transformation is initiated increases with decreasing grain size for both grain orientations (i.e., a higher initial resistance to transformation for smaller grains). In accordance with the expressions given in (9)–(11), the driving force

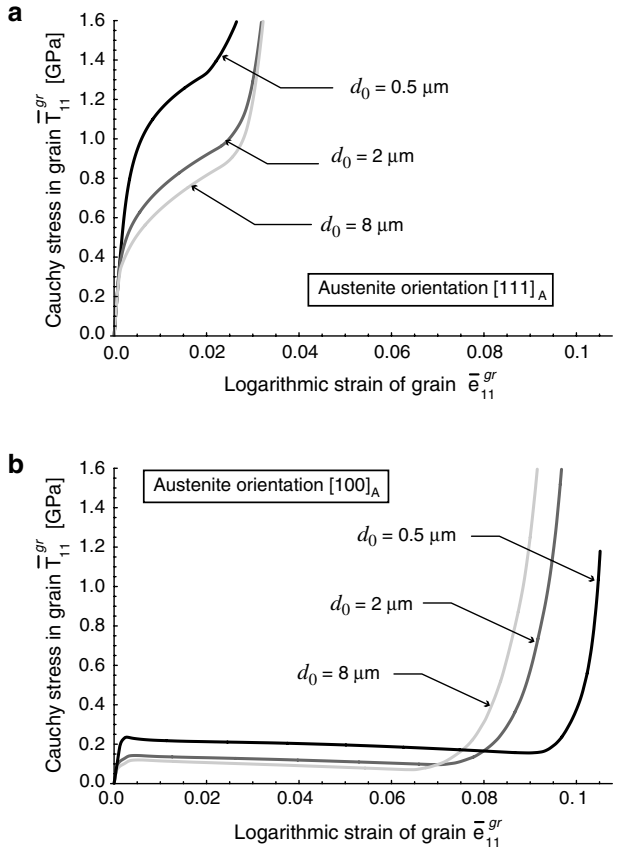

Fig. 4. Axial Cauchy stress $\overline{T}^{\mathrm{gr}}_{11}$ vs. axial logarithmic strain $\bar{e}^{\mathrm{gr}}_{11}$ averaged over grain of retained austenite: (a) grain orientation $[1\,1\,1]_A$; (b) grain orientation $[1\,0\,0]_A$.

available at the onset of transformation (when $\xi^{(\alpha)} = 0$) has a positive contribution from the resolved stress, a negative contribution from the mismatch in stiffnesses (since martensite is stiffer than austenite) and a negative contribution from the energy required to create interfaces. This latter term, which in view of (11) is equal to $-\chi/l_0$ at the beginning of the transformation, is shown in Table 2. For the largest grain analyzed ($d_0 = 8$ μm), the term $\chi/l_0 = 1$ MPa has a relatively small contribution compared to the net initial transformation resistance under isothermal conditions, i.e., $f_{\mathrm{cr}} - f_{\mathrm{th}} = 5$ MPa. However, for the smallest grain analyzed ($d_0 = 0.5$ μm), the term $\chi/l_0 = 16$ MPa dominates the onset of the transformation. Hence, the necessary work per unit volume to create interfaces in smaller grains is higher and thus the value of $f^{(\alpha)}$ required to initiate the transformation is higher.

As shown in Figs. 4a and b, the slopes of the stress–strain curves initially decrease as the austenite begins to transform into martensite but eventually increase as the transformation process stops. The deformation between these two inflection points in the stress–strain curves is approximately equal to the effective transformation strain in the axial direction. Here, the effective transformation strain is defined as the average axial transformation strain in the grain when the transformation process ends. For grains loaded in the $[1\,0\,0]_A$ direction, the effective transformation strain is considerably larger than for grains loaded in the $[1\,1\,1]_A$ direction and, therefore, the $[1\,0\,0]_A$-loaded grains show a softer response during transformation. As demonstrated in Turteltaub and Suiker (2005), under a *homogeneous* uniaxial deformation, the axial transformation strain is equal to 2.7% for a grain loaded in the $[1\,1\,1]_A$ direction and to 11% for a grain loaded in the $[1\,0\,0]_A$ direction. Figs. 4a and b illustrate that the effective axial transformation strains in the present simulations are below the values of the corresponding homogeneous uniaxial deformations for both grain orientations and all grain sizes.

As can be observed in Fig. 4a, for a grain loaded in the $[1\,1\,1]_A$ direction, the effective axial transformation strain *decreases* as the grain size *decreases*. In contrast, for the grains loaded in the $[1\,0\,0]_A$ direction, the effective axial transformation strain *increases* as the grain size *decreases*. The dependence of the effective transformation strain on the grain size is related to the deviation from a state of uniaxial stress inside the grain due to the triaxial stress state. A deviation from a state of uniaxial stress can be measured in terms of the lateral stresses $\overline{T}^{\mathrm{gr}}_{22}$ and $\overline{T}^{\mathrm{gr}}_{33}$. Based on the values of these stresses (not reported here), for $[1\,1\,1]_A$-loaded grains this deviation occurs at lower strain values for smaller grain sizes. This situation is reversed for grains loaded in the $[1\,0\,0]_A$ direction where the deviation from a uniaxial stress state occurs at lower strain values for larger grain sizes. A deviation from a state of uniaxial stress tends to activate additional transformation systems that are not optimally oriented with respect to a uniaxial deformation and, consequently, tend to lower the effective uniaxial transformation strain. In addition, as shown below in Section 3.3, the reduction in effective transformation strain for smaller grains loaded in the $[1\,1\,1]_A$ direction is amplified due to an incomplete phase transformation.

3.3. Size effects on rate of phase transformation

The evolution of the transformation, measured in terms of the average volume fraction of retained austenite $\bar{\xi}_A$, is shown as a function of the average axial logarithmic strain $\bar{e}_{11}$ in Figs. 5a and b for austenitic grains loaded in the $[1\,1\,1]_A$ and $[1\,0\,0]_A$ directions, respectively. For grains loaded in the $[1\,1\,1]_A$ direction, the rate of transformation $|\mathrm{d}\bar{\xi}_A/\mathrm{d}\bar{e}_{11}|$ is *lower* for *smaller* grain sizes while for grains loaded in the $[1\,0\,0]_A$ direction the transformation rate is *higher* for *smaller* grain sizes. In addition, it is interesting to observe that grains of austenite loaded in the $[1\,1\,1]_A$ direction do not fully transform into martensite; the amount of untransformed austenite increases as the grain size becomes smaller. This trend is in accordance with experimental

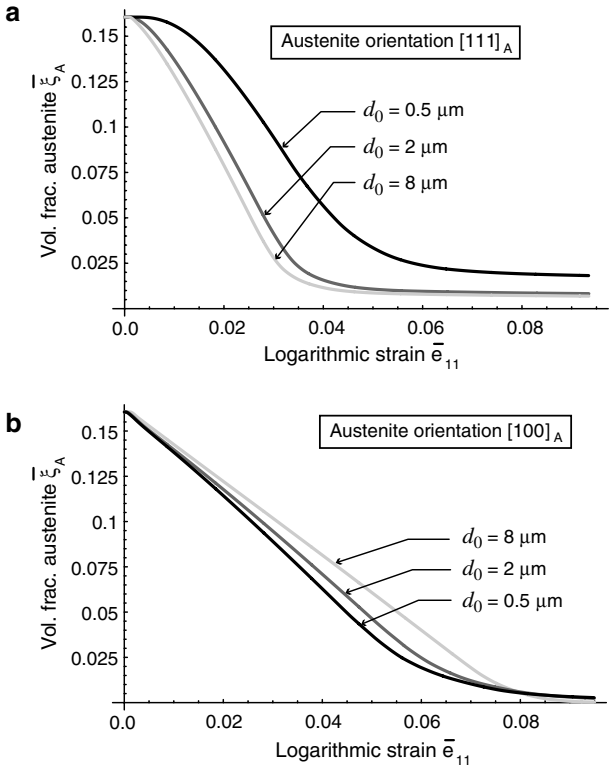

Fig. 5. Average volume fraction of austenite $\bar{\xi}_A$ as a function of the axial logarithmic strain $\bar{e}_{11}$ averaged over entire domain for several values of the grain size d_0: (a) grain orientation $[1\,1\,1]_A$; (b) grain orientation $[1\,0\,0]_A$.

results (Jeong et al., 1993; Bai et al., 1998). In contrast, since grains of austenite loaded in the $[1\,0\,0]_A$ direction are more favorably oriented for transformation, they fully transform into martensite, which occurs at about 10% strain for all grain sizes.

3.4. Size effects on strain partitioning

The grain-averaged axial strain $\bar{e}_{11}^{\mathrm{gr}}$ as a function of the axial strain averaged over the entire computational domain $\bar{e}_{11}$ is shown in Figs. 6a and b for grains loaded in the $[1\,1\,1]_A$ and $[1\,0\,0]_A$ directions, respectively. The strain partitioning curves plotted in Fig. 6a indicate that the grain deformation initially follows the overall strain during the transformation process. For larger grains, the strain in the grain $\bar{e}_{11}^{\mathrm{gr}}$ is closer to the overall strain $\bar{e}_{11}$. As the transformation process ends, the grains start to behave as hard inclusions (i.e., $\bar{e}_{11}^{\mathrm{gr}} < \bar{e}_{11}$). As opposed to grains loaded in the $[1\,1\,1]_A$ direction, smaller grains loaded in the $[1\,0\,0]_A$ direction can initially follow the overall strain $\bar{e}_{11}$ (slightly) closer than larger grains. For all grain sizes, the initial behavior of grains loaded in the $[1\,0\,0]_A$ direction corresponds to the response of a very soft inclusion (i.e., $\bar{e}_{11}^{\mathrm{gr}} > \bar{e}_{11}$). Only when the transformation process ends, the strain partitioning curves cross the equal-strain line and the grains start to behave as hard inclusions.

3.5. Size effects at the level of the whole computational domain

The response of the material averaged over the whole computational domain (axial Cauchy stress $\overline{T}_{11}$ as a function of the axial logarithmic strain $\bar{e}_{11}$) is shown in Figs. 7a and b for austenitic grains loaded in the $[1\,1\,1]_A$ and $[1\,0\,0]_A$ directions, respectively. The figures also include the results of a benchmark calculation where the whole domain is occupied by the ferrite-based material. This case is used as a reference to quantify the net

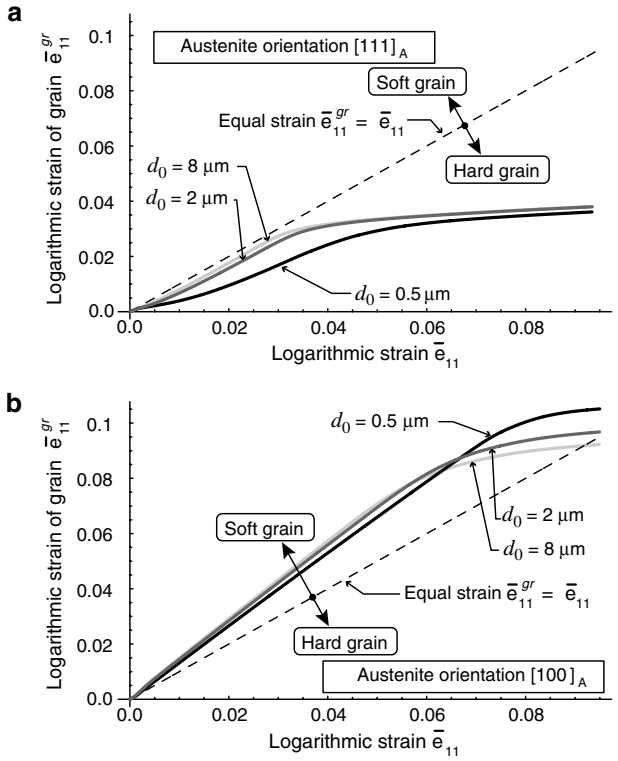

Fig. 6. Average logarithmic strain in grain $\bar{e}_{11}^{\mathrm{gr}}$ vs. average logarithmic strain $\bar{e}_{11}$ in entire domain for several values of the grain size d_0: (a) grain orientation $[1\,1\,1]_A$; (b) grain orientation $[1\,0\,0]_A$.

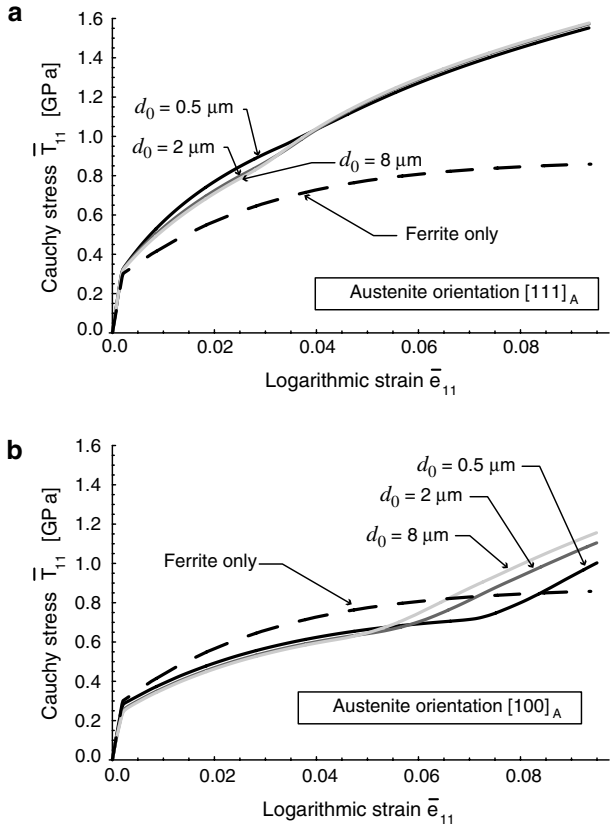

Fig. 7. Axial Cauchy stress $\overline{T}_{11}$ vs. axial logarithmic strain $\bar{e}_{11}$ averaged over entire domain: (a) grain orientation $[1\,1\,1]_A$; (b) grain orientation $[1\,0\,0]_A$.

effect of the grain of retained austenite on the effective constitutive response. As shown in Figs. 7a and b, grains loaded in the $[1\,1\,1]_A$ direction have a higher strength than the ferrite-based material, whereas grains loaded in the $[1\,0\,0]_A$ direction have initially a lower strength, although it eventually becomes higher as the transformation process ends. The difference in strength between the $[1\,1\,1]_A$- and $[1\,0\,0]_A$-loaded grains can be connected to, respectively, the hard and soft responses in those orientations during transformation (see Figs. 6a and b).

For both grain orientations, the strength of the material is initially higher for decreasing grain size. However, at higher strain levels (approximately above 4% for grains loaded in the $[1\,1\,1]_A$ direction and above 5% for grains loaded in the $[1\,0\,0]_A$ direction), the overall strength is slightly smaller for smaller grain sizes. The details of the influence of the grain size can be traced back to the grain-averaged behavior discussed in the previous sections. In general, the influence of the grain size on the effective response is far less significant than the influence of the grain orientation. Nonetheless, in view of the grain-averaged responses shown in Figs. 4a and b, it is anticipated that size effects will become more pronounced as the volume fraction of the austenite is increased.

4. Concluding remarks

In a multiphase carbon steel, the local mechanical response of a transforming grain of retained austenite strongly depends on the grain size. The surface energy term in the transformation model captures the increased resistance to transformation due to a reduction in the size of the austenitic grains, which is in agreement with experimental observations. Simulations show incomplete transformations for grains loaded in the $[1\,1\,1]_A$ direction, particularly as the grain size is reduced. In contrast, grains loaded in the $[1\,0\,0]_A$ direction fully

transform into martensite. Furthermore, for this orientation, the deformation in the austenite is more homogeneous for smaller grains, which results in a higher effective transformation strain.

The grain size effect is less noticeable in the overall response of a sample containing a grain of retained austenite embedded in a ferrite-based matrix. At this level of observation, the response depends primarily on volume fraction and grain orientation. However, it is expected that size effects will become more prominent in multiphase carbon steels with high volume fractions of retained austenite. The available experimental data for grain size effects in multiphase carbon steels is mainly related to transformation kinematics; additional experimental studies that quantify stress distributions are required to confirm the results predicted in the present study. Furthermore, it is relevant to mention that the transformation model does not include plastic deformation in the austenite nor damage due to the martensitic transformation. These effects are likely to play an important role at high strain levels. Nonetheless, the predictions of the current model can qualitatively capture the most relevant grain size effects during the initial stage of transformation.

Acknowledgements

This work is part of the research program of the Netherlands Institute for Metals Research (NIMR) and the Stichting voor Fundamenteel Onderzoek der Materie (FOM, financially supported by the Nederlandse Organisatie voor Wetenschappelijk Onderzoek (NWO)). The research was carried out under project number 02EMM20 of the FOM/NIMR program "Evolution of the Microstructure of Materials" (P-33).

References

Bai, D.Q., Di Chiro, A., Yue, S., 1998. Stability of retained austenite in a Nb microalloyed Mn–Si TRIP steel. Mater. Sci. Forum, 253–260.

Ball, J.M., James, R.D., 1987. Fine phase mixtures as minimizers of energy. Arch. Rat. Mech. An. 100 (1), 13–52.

Callen, H.B., 1985. Thermodynamics and an Introduction to Thermostatistics, second ed. John Wiley & Sons.

Christian, J.W., 2002. The Theory of Transformations in Metals and Alloys (Part II), third ed. Pergamon Press.

Furnémont, Q., Kempf, M., Jacques, P.J., Göken, M., Delannay, F., 2002. On the measurement of the nanohardness of the constitutive phases of TRIP-assisted multiphase steels. Mater. Sci. Eng. A 328 (1–2), 26–32.

Iwamoto, T., Tsuta, T., 2000. Computational simulation of the dependence of the austenitic grain size on the deformation behavior of TRIP steels. Int. J. Plast. 16 (7–8), 791–804.

Jacques, P.J., Ladrière, J., Delannay, F., 2001. On the influence of interactions between phases on the mechanical stability of retained austenite in transformation-induced plasticity multiphase steels. Metall. Mater. Trans. A 32, 2759–2768.

Jeong, W.C., Matlock, D.K., Krauss, G., 1993. Observation of deformation and transformation behavior of retained austenite in a 0.14C–1.2Si–1.5Mn steel with ferrite bainite austenite structure. Mater. Sci. Eng. A. 165 (1), 1–8.

Kruijver, S.O., Zhao, L., Sietsma, J., Offerman, S.E., van Dijk, N.H., Lauridsen, E.M., Margulies, L., Grigull, S., Poulsen, H.F., van der Zwaag, S., 2003. In situ observations on the mechanical stability of austenite in TRIP-steel. J. Phys. IV 104, 499–502.

Leal, R.H., Guimaraes, J.R.C., 1981. Microstructure evolution during mechanically induced martensitic-transformation in Fe–31-percent Ni–0.1-percent-C. Mater. Sci. Eng. 48 (2), 249–254.

Oliver, E.C., Withers, P.J., Daymond, M.R., Ueta, S., Mori, T., 2002. Neutron-diffraction study of stress-induced martensitic transformation in TRIP steel. Appl. Phys. A 74, S1143–S1145.

Olson, G.B., Cohen, M., 1975. Kinetics of strain-induced martensitic nucleation. Metall. Trans. A 6 (4), 791–795.

Perlade, A., Bouaziz, O., Furnémont, Q., 2003. A physically based model for TRIP-aided carbon steels behaviour. Mater. Sci. Eng. A 356 (1–2), 145–152.

Rao, B.V.N., Rashid, M.S., 1997. Direct observations of deformation-induced retained austenite transformation in a vanadium-containing dual-phase steel. Mater. Char. 39 (2–5), 435–453.

Reisner, G., Werner, E.A., Fischer, F.D., 1998. Micromechanical modeling of martensitic transformation in random microstructures. Int. J. Solids Struct. 35 (19), 2457–2473.

Sugimoto, K.I., Kobayashi, M., Yasuki, S.I., 1997. Cyclic deformation behavior of a transformation-induced plasticity-aided dual-phase steel. Metall. Mater. Trans. A 28, 2637–2644.

Suiker, A.S.J., Turteltaub, S., 2005. Computational modelling of plasticity induced by martensitic phase transformations. Int. J. Numer. Methods Eng. 63 (12), 1655–1693.

Tjahjanto, D.D., Turteltaub, S., Suiker, A.S.J., van der Zwaag, S., 2006. Modelling of the effects of grain orientation on transformation-induced plasticity in multiphase carbon steels. Modell. Simul. Mater. Sci. Eng. 14 (4), 617–636.

Turteltaub, S., Suiker, A.S.J., 2005. Transformation-induced plasticity in ferrous alloys. J. Mech. Phys. Solids 53 (8), 1747–1788.

Turteltaub, S., Suiker, A.S.J., 2006. A multiscale thermomechanical model for cubic to tetragonal martensitic phase transformations. Int. J. Solids Struct. 43 (14–15), 4509–4545.

Umemoto, M., Yoshitake, E., Tamura, I., 1983. The morphology of martensite in Fe–C, Fe–Ni–C and Fe–Cr–C alloys. J. Mater. Sci. 18 (10), 2893–2904.

Wang, J.J., van der Zwaag, S., 2001. Stabilization mechanisms of retained austenite in transformation-induced plasticity steel. Metall. Mater. Trans. A 32 (6), 1527–1539.

Wechsler, M.S., Lieberman, D.S., Read, T.A., 1953. On the theory of the formation of martensite. Trans. Am. Inst. Miner. Metall. Eng. 197 (11), 1503–1515.